Monodisperse Noble-Metal Nanoparticles and Their Surface Enhanced Raman Scattering Properties

Chengmin Shen, Chao Hui, Tianzhong Yang, Congwen Xiao, Jifa Tian, Lihong Bao, Shutang Chen, Hao Ding, and Hongjun Gao*

Beijing National Laboratory for Condensed Matter Physics, Institute of Physics, Chinese Academy of Sciences, 100190 Beijing, China

Received March 27, 2008. Revised Manuscript Received September 21, 2008

Monodisperse Au, Ag, and Au_3Pd nanoparticles (NPs) with narrow size distribution are prepared by direct reaction of the related metal salt with oleylamine in toluene. Oleylamine serves as both a reducing agent and a surfactant in the synthesis. The sizes and shape of these NPs are tuned by reaction temperatures. The hydrophobic oleylamine-coated NPs can be made water soluble by replacing oleylamine with 3-mercaptopropionic acid. Both surface plasmonic resonance (SPR) and surface enhanced Raman scattering (SERS) observed from the Au and Ag NPs are found to be NP size- and surface-dependent.

Introduction

Au and Ag based noble metal nanoparticles (NPs) have attracted considerable interest due to their potential applications in catalysis, biolabeling, and photonics.[1−10] Their size, size distribution, and morphology control have been the key to the understanding of the optical and surface properties. Conventionally, Au and Ag NPs are made either by Faraday method in aqueous solutions via sodium citrate reduction of $HAuCl_4$[11−17] or by Brust's and Schiffrin's liquid−liquid two phase method in an organic phase by sodium borohydride reduction of $AuC1_4^{-1}$ or $AgNO_3$ in the presence of an alkanethiol.[18−23] To better control the NP size and size distribution, the synthesis is also performed in a single organic solvent via using strong or mild reducing agent to reduce different gold compound.[24−33] Despite all these efforts made for the synthesis, the quality of the Au and Ag NPs is still far from well controlled, and the NPs prepared often have broad size and shape distribution, unsuitable for constructing highly ordered superlattice arrays and for deep understanding of the physical and chemical properties.[34−40]

Here, we report a general one-pot organic phase synthesis of monodisperse noble metal NPs via the reaction between

* Corresponding author. E-mail: hjgao@aphy.iphy.ac.cn.

(1) Xia, Y. N.; Halas, N. J. *MRS Bull.* **2005**, *30*, 338–348.
(2) Sau, T. K.; Murphy, C. J. *J. Am. Chem. Soc.* **2004**, *126*, 8648–8649.
(3) Hashmi, A. S. K. *Chem. Rev.* **2007**, *107*, 3180–3211.
(4) Cho, J. K.; Najman, R.; Dean, T. W.; Ichihara, O.; Muller, C.; Bradley, M. *J. Am. Chem. Soc.* **2006**, *128*, 6276–6277.
(5) Orendorff, C. J.; Sau, T. K.; Murphy, C. J. *Small* **2006**, *2*, 636–639.
(6) Merican, Z.; Schiller, T. L.; Hawker, C. J.; Fredericks, P. M.; Blakey, I. *Langmuir* **2007**, *23*, 10539–10545.
(7) Mulvaney, S. P.; Musick, M. D.; Keating, C. D.; Natan, M. J. *Langmuir* **2003**, *19*, 4784–4790.
(8) Zhang, Z. F.; Cui, H.; Lai, C. Z.; Liu, L. *J. Anal. Chem.* **2005**, *77*, 3324–3329.
(9) Manea, F.; Houillon, F. B.; Pasquato, L.; Scrimin, P. *Angew. Chem., Int. Ed.* **2004**, *43*, 6165–6169.
(10) Hashmi, A. S. K.; Hutchings, G. J. *Angew. Chem., Int. Ed.* **2006**, *45*, 7896–7936.
(11) Faraday, *Philos. Trans.* **1857**, 145–181.
(12) Xiong, Y. J.; Washio, I.; Chen, J. Y.; Sadilek, M.; Xia, Y. N. *Angew. Chem., Int. Ed* **2007**, *46*, 4917–4921.
(13) Chen, J. Y.; McLellan, J. M.; Siekkinen, A.; Xiong, Y. J.; Li, Z. Y.; Xia, Y. N. *J. Am. Chem. Soc.* **2006**, *128*, 14776–14777.
(14) Datta, K. K. R.; Eswaramoorthy, M.; Rao, C. N. R. *J. Mater. Chem.* **2007**, *17*, 613–615.
(15) Xiong, Y. J.; Wiley, B.; Chen, J. Y.; Li, Z. Y.; Yin, Y. D.; Xia, Y. N. *Angew. Chem., Int. Ed.* **2005**, *44*, 7913–7917.
(16) Njoki, P. N.; Luo, J.; Wang, L. Y.; Maye, M. M.; Quaizar, H.; Zhong, C. J. *Langmuir* **2005**, *21*, 1623–1628.
(17) Herricks, T.; Chen, J. Y.; Xia, Y. N. *Nano Lett.* **2004**, *4*, 2367–2371.
(18) Brust, M.; Walker, M.; Bethell, D.; Schiffrin, D. J.; Whyman, R. *Chem. Commun.* **1994**, 801–802.
(19) (a) Brown, L. O.; Hutchison, J. E. *J. Am. Chem. Soc.* **1999**, *121*, 882–883. (b) Brown, L. O.; Hutchison, J. E. *J. Phys. Chem. B* **2001**, *105*, 8911–8916.
(20) Chen, S. W.; Huang, K.; Stearns, J. A. *Chem. Mater.* **2000**, *12*, 540–547.
(21) (a) Shen, C. M.; Su, Y. K.; Yang, H. T.; Yang, T. Z.; Gao, H.-J. *Chem. Phys. Lett.* **2003**, *373*, 39–45. (b) He, S. T.; Yao, J. N.; Jiang, P.; Shi, D. X.; Zhang, H. X.; Xie, S. S.; Pang, S. J.; Gao, H.-J. *Langmuir* **2001**, *17*, 1571–1575.
(22) Harfenist, S. A.; Wang, Z. L.; Alvarez, M. M.; Vezmar, I.; Whetten, R. L. *J. Phys. Chem.* **1996**, *100*, 13904–13910.
(23) (a) Templeton, A. C.; Wuelfing, M. P.; Murray, R. W. *Acc. Chem. Res.* **2000**, *33*, 27–36. (b) Leff, D. V.; Brandt, L.; Heath, J. R. *Langmuir* **1996**, *12*, 4723–4730.
(24) Schulz-Dobrick, M.; Sarathy, K. V.; Jansen, M. *J. Am. Chem. Soc.* **2005**, *127*, 12816–12817.
(25) Jana, N. R.; Peng, X. G. *J. Am. Chem. Soc.* **2003**, *125*, 14280–14281.
(26) Rowe, M. P.; Plass, K. E.; Kim, K.; Kurdak, C.; Zellers, E. T.; Matzger, A. J. *Chem. Mater.* **2004**, *16*, 3513–3517.
(27) Zheng, N. F.; Fan, J.; Stucky, G. D. *J. Am. Chem. Soc.* **2006**, *128*, 6550–6551.
(28) Yee, K.; Jordan, R.; Ulman, A.; White, H.; King, A.; Rafailovich, M.; Sokolov, J. *Langmuir* **1999**, *15*, 3486–3491.
(29) Shi, C. S.; Tian, L. F.; Wu, L. L.; Zhu, J. *J. Phys. Chem. C* **2007**, *111*, 1243–1247.
(30) Ren, J. T.; Tilley, R. D. *Small* **2007**, *3*, 1508–1512.
(31) Hiramatsu, H.; Osterloh, F. E. *Chem. Mater.* **2004**, *16*, 2509–2511.
(32) Aslam, M.; Fu, L.; Su, M.; Vijayamohanan, K.; Dravid, V. P. *J. Mater. Chem.* **2004**, *14*, 1795–1797.
(33) Liu, X.; Wang, J. H.; Atwater, M.; Dai, Q.; Zou, J. H.; Brennan, J. P.; Huo, Q. *J. Nanosci. Nanotechnol.* **2007**, *7*, 3126–3133.
(34) Yamamoto, M.; Nakamoto, M. *J. Mater. Chem.* **2003**, *13*, 2064–2065.
(35) Kim, S. W.; Park, J.; Jang, Y. J.; Chung, Y. H.; Hwang, S. J.; Hyeon, T. *Nano Lett.* **2003**, *3*, 1289–129.
(36) Yang, H. T.; Shen, C. M.; Su, Y. K.; Yang, T. Z.; Gao, H.-J. *Appl. Phys. Lett.* **2003**, *82*, 4729–4731.
(37) Rogach, A. L. *Angew. Chem., Int. Ed.* **2004**, *43*, 148–149.
(38) Xu, Z. C.; Shen, C. M.; Xiao, C. W.; Yang, T. Z.; Zhang, H. R.; Li, J. Q.; Li, H. L.; Gao, H.-J. *Nanotechnology* **2007**, *18*, 115608–115612.
(39) Park, J.; Lee, E.; Hwang, N. M.; Kang, M.; Kim, S. C.; Hwang, Y.; Park, J. G.; Noh, H. J.; Kim, J. Y.; Park, J. H.; Hyeon, T. *Angew. Chem., Int. Ed.* **2005**, *44*, 2872–2877.

10.1021/cm800882n CCC: $40.75
Published on Web 10/29/2008

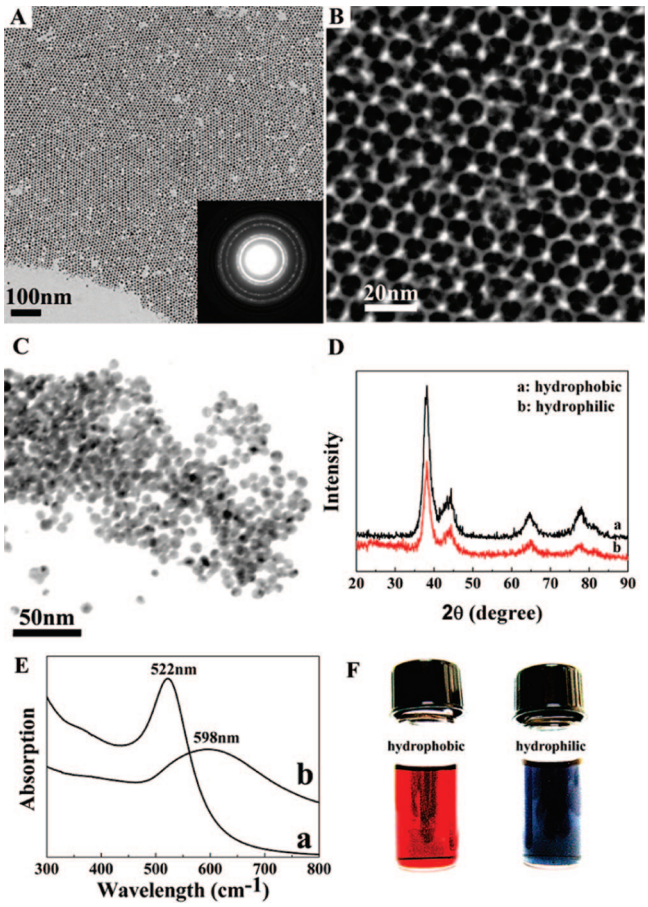

Figure 1. TEM images and XRD patterns of hydrophobic Au NPs and hydrophilic Au NPs. (a) Large area TEM image of oleylamine-capped Au NPs; (b) superlattice structure of oleylamine-capped Au NPs. (c) TEM image of 3-mercaptopropionic acid-capped Au NPs. (d) XRD patterns of hydrophobic and hydrophilic Au NPs. (e) UV−vis spectra of hydrophobic and hydrophilic of Au NPs. (f) Optical photograph of hydrophobic and hydrophilic of Au NP samples dissolved in heptane and water, respectively.

the related metal salt and oleylamine. Au NPs were prepared by reducing $HAuCl_4 \cdot 4H_2O$ in the toluene solution of oleylamine. The sizes of the Au NPs were tuned from 8.5 to 23.8 nm by reaction temperatures. Monodisperse Ag or AuPd NPs were also made similarly via the reduction of $AgNO_3$ or coreduction of $HAuCl_4$ and $Pd(acac)_2$ with the AuPd composition controlled by the molar ratio of these two salts. The monodipserse Au and Ag NPs self-assembled into the superlattice arrays and had the surface plasmonic resonance (SPR) band at 523 nm and 407 nm in heptane, respectively. The SPR band of the nanoscale Au was blue-shifted to 7 nm in Au_3Pd NPs and red-shifted to 598 nm upon the replacement of oleyalmine around the Au NPs with 3-mercaptopropionic acid. The oleylamine-capped Au and Ag NPs also exhibited good surface-enhanced Raman scattering (SERS) effect on the model molecule Rhodamine B or 2-naphthalenethiol and the larger Au NPs had higher SERS peak intensity. The work offers a general approach to the noble metal NPs that may be important for optical applications.

(40) Yang, T. Z.; Shen, C. M.; Li, Z. A.; Zhang, H. R.; Xiao, C. W.; Chen, S. T.; Xu, Z. C.; Shi, D. X.; Li, J. Q.; Gao, H.-J. *J. Phys. Chem. B* **2005**, *109*, 23233–23236.

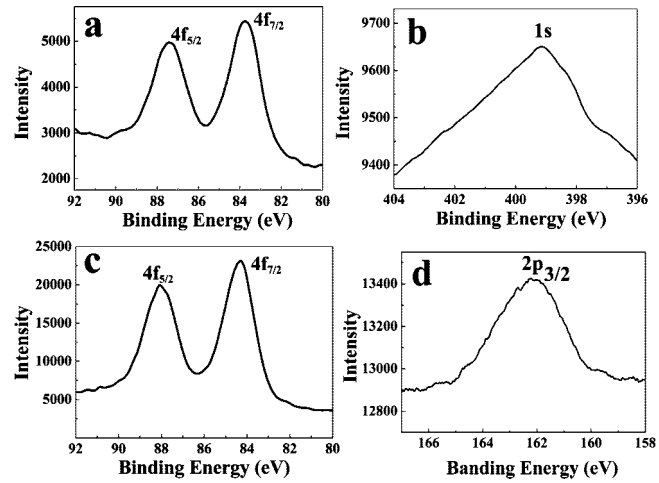

Figure 2. XPS spectra of hydrophobic and hydrophilic Au NPs; (a) Au in hydrophobic; (b) N in hydrophobic; (c) Au in hydrophilic; (d) S in hydrophilic.

Experimental Section

Materials. $HAuCl_4 \cdot 4H_2O$ and toluene (analysis degree) were purchased from Beijing Chemical reagents Co. Oleylamine (>70%), 2-naphthalenethiol, and 4-mercaptobenzoic acid were obtained from Aldrich. Palladium acetylacetonate (>99%), silver nitrate (>99%), and 3-mercaptopropionic acid were purchased from ACROS. Rhodamine B is obtained from Sigma. All other reagents were used without further purification.

Synthesis of Hydrophobic 8.5 nm Au NPs. A total of 1 mmol of $HAuCl_4 \cdot 3H_2O$ and 5 mL (10 mmol) of oleylamine were mixed with 50 mL toluene in a 100 mL flask. Under nitrogen protection, the mixture was heated to 65 °C under magnetic stirring. The solution was kept at this temperature for 6 h and cooled down to room temperature. A total of 50 mL of ethanol was added into the solution, and the suspension was centrifuged at 6000 rpm for 3 min. The supernatant was discarded. The NPs were redispersed in heptane to give a red dispersion.

Synthesis of Hydrophilic 8.5 nm Au NPs. A total of 2 mL of the heptane dispersion of the oleylamine-capped Au NPs (17 mg/mL), 10 mL of heptane, and 5 mL of 3-mercaptopropionic acid were mixed into a 50 mL flask. The resultant solution was stirred overnight at room temperature. The solution was centrifuged at 6000 rpm for 3 min, and the precipitation was washed by acetone three times. The final product was dissolved in deionized water to give a blue dispersion.

Synthesis of 13 nm Ag NPs. A total of 0.5 mmol of $AgNO_3$ and 2 mL of oleylamine were dissolved in 50 mL of toluene in a 100 mL flask. The mixture was heated to 110 °C under nitrogen flow and kept at this temperature for 6 h before it was cooled down to room temperature. A total of 50 mL of ethanol was added into the solution, and the suspension was centrifuged at 6000 rpm for 3 min. The supernatant was discarded. The precipitation was redissolved in heptane to give a brown-yellow dispersion.

Synthesis of 7 nm Au_3Pd NPs. Under a nitrogen flow, 0.66 mmol of $HAuCl_4 \cdot 4H_2O$, 0.33 mmol of $Pd(acac)_2$, 10 mL of oleylamine, and 50 mL of toluene were mixed in a 100 mL flask. The mixture was then slowly heated with stirring at 80 °C for 1 h. Then the reaction temperature was raised to 100 °C for 1 h. The solution was cooled down room temperature by removing the heating source. A total of 50 mL of enthanol was added, and the product was separated by centrifugation (6000 rmp for 5 min). The product was then dispersed in heptane.

Au and Ag NP Assembly for SERS Study. A total of 1.0 mL of heptane dispersion of the hydrophobic Au NPs was dropped onto

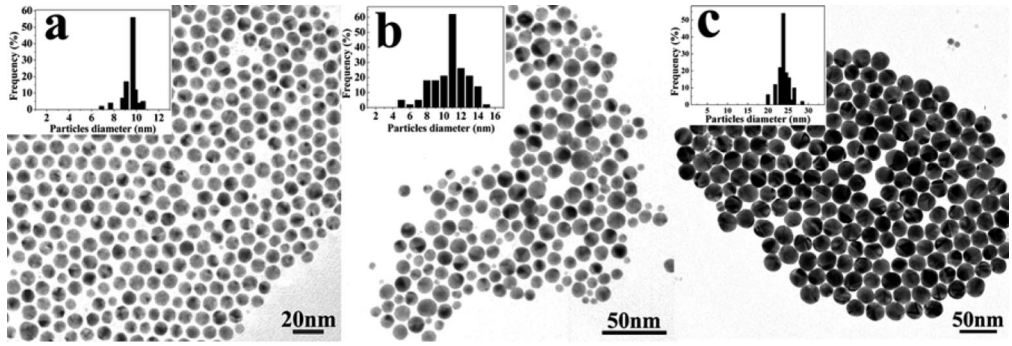

Figure 3. TEM images of Au NPs prepared in toluene solution at different temperatures: (a) 75 °C; (b) 95 °C; and (c) 115 °C.

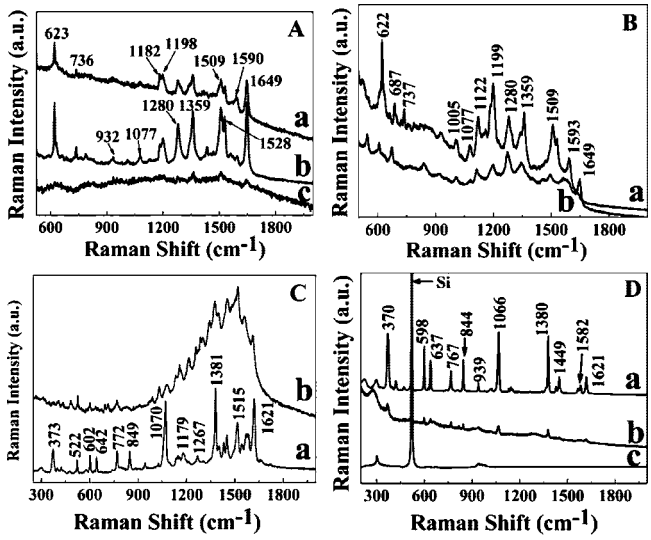

Figure 4. SERS spectra of hydrophobic and hydrophilic of Au NPs using Rhodamine B (A and B) and 2-naphthalenethiol (C and D) as model molecule at different excitation sources. (a) SERS spectrum of hydrophobic Au NPs, (b) SERS spectrum of hydrophilic Au NPs; (A-c) Raman scattering spectrum of Rhodamine B molecule; (D-c) Raman scattering spectrum of 2-naphthalenethiol molecule. (A and C) 633 nm used as excitation source; (B and D) 785 nm used as excitation source.

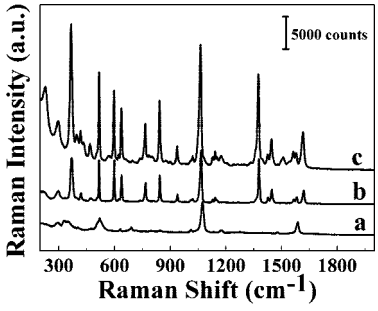

Figure 5. SERS spectra of different size Au NPs using 2-naphthalenethiol as model molecule under 785 laser line: (a) 9.5 nm; (b) 10.8 nm; (c) 23.8 nm.

the 1 × 1 cm^2 Si(111) wafer and dried under ambient conditions. Then, this Si wafer was put into a 5 mL beaker containing 0.8 mL of 1 × 10^{-3} M Rhodamine B aqueous solution or 1 × 10^{-3} M 2-naphthalenethiol enthanol solution. The Au NPs covered Si wafer was washed three times with ethanol and dried in air. For comparison, the same procedure was also applied on the Si substrate modified only with Rhodamine B or 2-Naphthalenethiol. Similar to the Au NPs, 1.0 mL of heptane dispersion of oleylamine-capped Ag NPs was dropped on the surface of the Si substrate and put into 1 × 10^{-3} M 4-mercaptobenzoic acid enthanol solution. The Si wafer was washed three times with ethanol and dried in air.

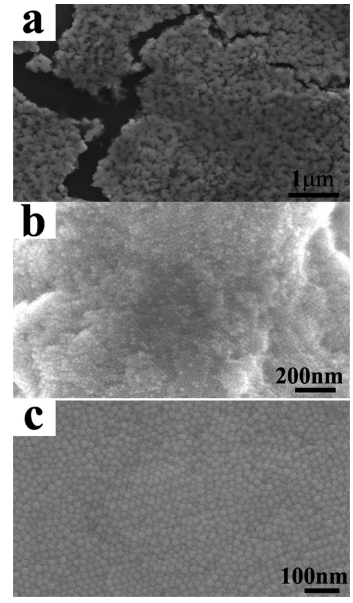

Figure 6. SEM images of different size Au NPs deposited on the Si substrate: (a) 9.5 nm; (b) 10.8 nm; (c) 23.8 nm.

Characterization of NPs. X-ray diffraction pattern of the NPs nanoparticle assembly was collected on a Rigaku D/MAX 2400 X-ray diffractometer with Cu Kα radiation (λ = 1.5406 Å). The UV−vis spectrum was recorded at room temperature on a Carry 1E ultraviolet−visible spectrometer using 1-cm quartz cuvettes. The surface enhanced Raman spectrum was recorded on the Raman system YJ-HR800 with confocal microscopy. The solid-state diode laser (633 nm or 785 nm) was used as an excited source. The laser power on the samples was kept with 0.9 mW (633 nm) and 0.07 mW (785 nm). X-ray photoelectron spectra were obtained on the ESCA LAB5 X-ray photoelectron spectrometer with the monochromatic Mg X-ray. Transmission electron microcopy (TEM) images were acquired with Tecnai-20 (PHILIPS Cop) at 120 kV.

Results and Discussion

Preparation of Hydrophobic and Hydrophilic Au NPs. Figure 1 presents the TEM images of the Au NPs synthesized in this work. It can be seen that the oleylamine-capped Au NPs have uniform size at 8.5 nm and narrow size distribution (<5% standard deviation), and self-assembly of these particles gives hexagonal close packed arrays. The selective area electron diffraction (SAED) pattern of the 8.5 nm Au NPs is shown in the inset of Figure 1A with the diffraction rings corresponding to the (111), (200), (220), and (311) planes from the face-centered-cubic (fcc) Au

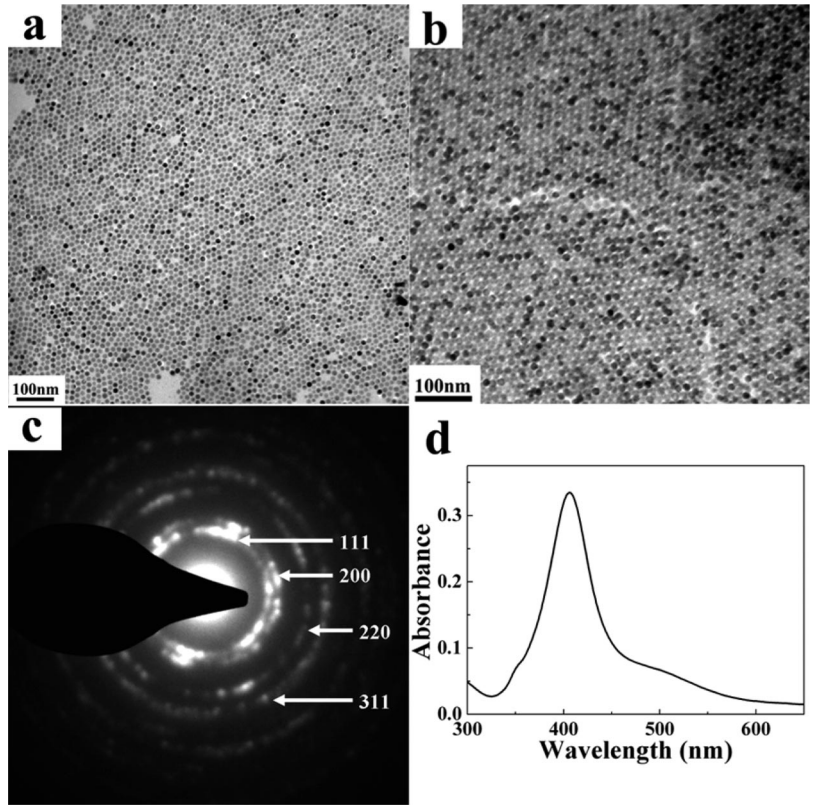

Figure 7. TEM images of 13 nm Ag NPs prepared in toluene solution; (a) monolayer film; (b) superlattices structure; (c) SAED pattern of Ag nanoparticle; and (d) UV−vis spectrum of Ag NPs.

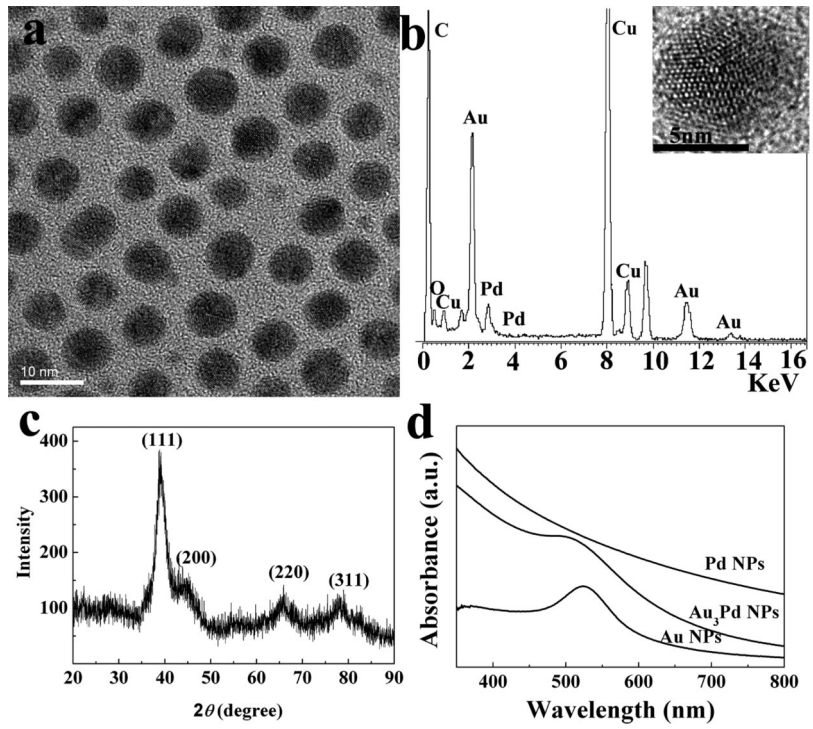

Figure 8. (a) TEM images of 7 nm Au_3Pd alloy NPs prepared in toluene solution; (b) XRD pattern of Au_3Pd alloy; (c) EDX pattern of Au_3Pd alloy; (d) UV−vis spectra of Au_3Pd alloy NPs.

structure. The oleylamine-capped hydrophobic Au NPs are transformed into water soluble Au NPs by replacing oleylamine with 3-mercaptopropionic acid. The −SH group in mercaptopropionic acid binds to Au, and −COOH surrounds the Au NPs. Figure 1C shows the TEM image of the hydrophilic Au NPs. Comparing with Figure 1A,C, we can see that there is no size and morphology change during the ligand exchange process. XRD patterns of both hydrophobic

(41) Chen, Z. T.; Gao, L. *Mater. Res. Bull.* **2007**, *42*, 1657–1661.

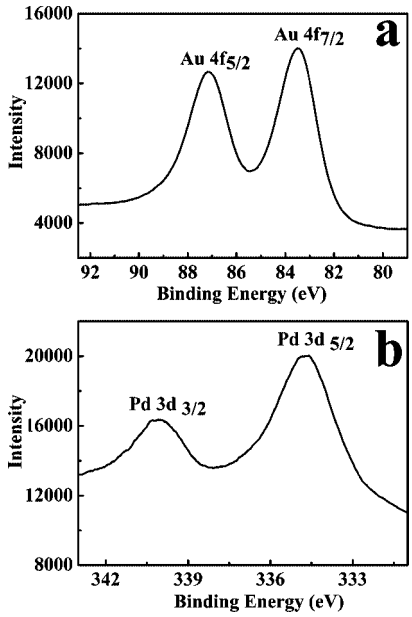

Figure 9. XPS spectra of d Au_3Pd alloy NPs prepared in toluene solution: (a) Au; (b) Pd.

and hydrophilic Au NPs are given in Figure 1D, confirming that the Au NPs in both cases have the fcc structure (JCPDS no. 04-0784). The UV−vis spectra of the hydrophobic and hydrophilic Au NPs are shown in the Figure 1E. The characteristic SPR band of the Au NPs capped with different ligands is located at 523 nm and 598 nm (Figure 1E). The absorption peak for the hydrophilic Au NPs is red-shifted, and the color of the dispersion turns from red into deep-blue (Figure 1F). This red-shift is likely caused by the partial aggregation of the Au NPs in water as observed in Figure 1C. This is consistent with what has been reported.[29,31,32] To better understand the surface environment of hydrophobic and hydrophilic Au NPs, we used X-ray photoelectron spectroscopy (XPS) to investigate the interaction of nitrogen and sulfur atoms on the surface of Au particles after surfactant exchange. Figure 2 shows the XPS spectra of hydrophobic and hydrophilic Au NPs. Two peaks are observed at 87.4 and 83.7 eV in the oleylamine-capped Au NPs, corresponding to the binding energies of $4f_{5/2}$ and $4f_{7/2}$, respectively. This is in agreement with the XPS spectra of the other alkylamine-capped Au NPs.[23b] Compared to the hydrophobic Au NPs, the 4f binding energies of the hydrophilic Au NPs shift to higher values from 87.4 and 83.7 eV to 88.1 and 84.4 V. This shift proves that the S−Au bond is stronger than the NH_2−Au bond.[21]

Reaction Temperature Effect on Size of Au NPs. Reaction temperature played a key role in nanoparticle size control. Figure 3 shows the TEM images of the Au NPs prepared at different temperatures. The size of the Au NPs is 9.5 nm (6.3% std. dev.) at 75 °C, 10.8 nm (12%, std. dev.) at 95 °C, and 23.8 nm (12%, std. dev.) at 115 °C, respectively. The higher reaction temperature results in a faster Au^{3+} reduction and growth process, producing large size NPs. [27,41] At lower reaction temperature (65 °C), the reduction is slowed down and the nucleation process overruns the growth process, yielding small particles.

SERS Study of the Au NPs. The SERS of the hydrophobic and hydrophilic Au NPs was investigated using 1×10^{-3} M Rhodamine B and 1×10^{-3} M 2-naphthalenetiol as model molecules. The excitation sources were 633 nm (laser power 0.9 mW) and 785 nm (laser power 0.07 mW) from a diode laser. Figure 4A,B show the SERS spectra of Rhodamine B adsorbed on hydrophobic and hydrophilic Au NPs at different excitation sources. The Raman peaks of hydrophobic and hydrophilic Au NPs display evident enhancement, compared with that from the pure Rhodmaine B (Figure 4A-c). The major bands of Rhodamine B molecule observed in two samples (Figure 4A) using 633 nm as the laser exciting line was also found under 785 nm (Figure 4B), indicating that Rhodamine B molecules are adsorbed on the surface of Au NPs.[6] However, the intensity of the SERS spectra is different between the hydrophilic Au NPs and hydrophobic ones under two exciting laser sources. Under 633 nm excitation, the SERS from the hydrophilic Au NPs is stronger than that from the hydrophobic ones. This is caused by the overlap between the exciting laser line and the SPR band of the hydrophilic particles at 598 nm. When the 785 nm laser exciting line is used, the SERS of the two samples are also enhanced, but the enhancement from the hydrophilic Au particles is evidently weaker than that from the hydrophobic one due to the difference in the exciting line and the SPR absorption of the hydrophilic particles. We also measured the SERS of the hydrophobic and hydrophilic Au NPs using 2-naphthalenethiol as a model molecule. The SERS spectra are shown in Figure 4C,D. Different from that of the Rhodamine B Au NPs, the SERS signals of the 2-naphthalenethiol-hydrophilic Au NPs are weaker in this case than that of the hydrophobic. Clearly, this is due to the chemical binding between −SH in 2-naphthalenethiol and the oleylamine-capped Au NPs, as confirmed from the Raman singlet at about 370 cm^{-1} (Figure 4C-a,D-a) that can be designated to one of the vibrational modes of the C−S bond upon coordination to the Au surface.[29] For hydrophilic Au NPs, 2-naphthalenethiol molecule has much less effect on the SERS due to the prebinding of the thiol molecule from 3-mercaptopropionic acid.

Size effect of the Au NPs on SERS. The SERS intensity is dependent on the sizes of the Au NPs. Figure 5 shows the SERS spectra of the Au NPs with different sizes (1×10^{-3} M 2-naphthalenethiol as model molecule). It can be seen that the SERS intensity of the 23.8 nm Au NPs is 9 times higher than that of the 9.5 nm Au NPs. This increase in SERS signal with Au NP sizes is in agreement with what is reported in Au NPs and Au nanohole arrays.[42,43] The larger Au NPs tend to form the larger area ordered superlattice structure on the Si substrate, as shown in Figure 6. The close packing of the Au NPs in a large area assembly can lead to a strong interparticle plasmon coupling and therefore the enhanced SERS.[44,45]

(42) Yu, Q. M.; Guan, P.; Qin, D.; Auen, G.; Wallace, P. M. *Nano Lett.* **2008**, *8*, 1923–1928.
(43) Kim, K.; Lee, H. B.; Lee, J. W.; Park, H. K.; Shin, K. S. *Langmuir* **2007**, *24*, 7178–7183.
(44) Sabur, A.; Havel, M.; Gogotsi, Y. *J. Raman Spectrosc.* **2008**, *39*, 61–67.

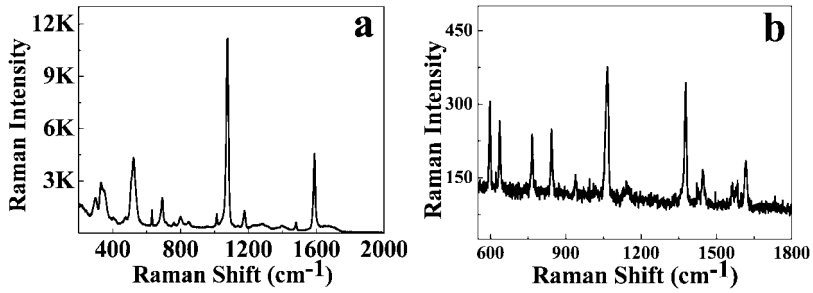

Figure 10. SERS spectra of Ag and Au_3Pd alloy NPs prepared in toluene solution: (a) Ag; (b) Au_3Pd alloy.

Preparation of Silver and Alloy NPs. The current synthesis can be readily extended to the preparation of other noble metal and alloy NPs. The 13 nm Ag NPs were obtained using $AgNO_3$ in oleylamine−toluene solution at 110 °C. Figure 7 shows the TEM images of Ag NPs. These NPs have narrow size distribution and can self-assemble into monolayer (Figure 7a) and multilayer superlattices (Figure 7b). The selective area electron diffraction pattern (Figure 7c) shows that the diffraction rings are from the (111), (200), (220), and (311) planes in the fcc Ag. The SPR band of the 13 nm Ag NPs appeared at 407 nm (Figure 7d). The good symmetric absorption peaks imply that the size of the NPs is very uniform.[21]

Using similar reaction conditions, we have also made monodisperse Au_3Pd NPs using 0.33 mmol Pd $(acac)_2$ and 0.67 mmol $HAuCl_4 \cdot 4H_2O$ as precursors. Figure 8a shows the TEM images of the 7 nm Au_3Pd NPs. The 3/1 Au/Pd was confirmed by EDX (Figure 8b). The HRTEM image of the Au_3Pd NPs in the inset of Figure 8b reveals good crystallinity of the particle. XRD patterns of the Au_3Pd NPs (Figure 8c) show the diffraction peaks at 38.8, 44.8, 65.9, and 77.9, corresponding to the (111), (200), (220), and (311) planes of the Au_3Pd NPs. These peaks are shifted away from those of the standard Au (JCPDS 04-0784) and palladium (JCPDS 46-1043), indicating that Au_3Pd alloy is indeed formed. Comparing with that of the Au NPs, the SPR band of the Au_3Pd alloy NPs is blue-shifted, proving that the optical properties of the NPs can be tuned by controlled composition in alloy NPs. The XPS spectra of the Au_3Pd NPs in the Au 4f and Pd 3d regions are shown in Figure 9. Two peaks locate at 87.1 eV and 83.5 eV corresponded to Au^0, while peaks at 340.1 and 334.7 eV are from Pd. The binding energy in Au_3Pd NPs is lower than that of the Au (87.67 eV and 84.0 eV) and Pd (335.1 eV and 340.36 eV).

We measured the SERS spectrum of the 13 nm Ag NPs using 1×10^{-3} M 4-mercaptobenzoic acid as a model molecule. The enhancement can be seen in Figure 10a. Similar to that in Au NPs, this enhancement is due to the formation of a large area Ag nanoparticle superlattice [Supporting Information and refs 29 and 42]. Figure 10b is the SERS spectrum of the Au_3Pd NPs. The characteristic Raman peaks from 1×10^{-3} M 2-naphthenethiol is detected, indicating that the AuPd alloy NPs may also be used in SERS. Detailed studies in SERS of the Ag NPs and the Au_3Pd NPs are underway.

Conclusions

A facile one-pot organic synthesis of Au, Ag, and Au_3Pd NPs with narrow size distribution is reported. The oleylamine serves as both a surfactant and a reducing agent. The size of the NPs is tuned through the reaction temperatures. These NPs are SERS active and this activity is dependent on the surface coating and the size of the particles. Through size control and surface modification, the optical properties of these monodisperse NPs should be readily optimized for potential highly sensitive optical detections.

Acknowledgment. The work was supported by the National Natural Science Foundation of China (Grant 60571045), National "863" Project of China (Grant 2007AA03Z305), and CAS/ SAFEA international cooperation team.

Supporting Information Available: Preparation of Pd NPs, TEM image of 8.5 nm hydrophilic Au NPs, SEM image of 13 nm Ag NPs deposited on the silicon substrate, TEM image of Pd NPs, and XRD of oleylamine-capped Pd NPs (PDF). This material is available free of charge via the Internet at http://pubs.acs.org.

CM800882N

(45) Çlha, M. C.; Kahraman, M.; Tokman, N.; Türkoğlu, G. *J. Phys. Chem. C* **2008**, *112*, 10338–10343.